nature chemical biology

ARTICLES

https://doi.org/10.1038/s41589-020-0548-3

Check for updates

Pyridoxal-5′-phosphate-dependent alkyl transfer in nucleoside antibiotic biosynthesis

Zheng Cui[1], Jonathan Overbay[1], Xiachang Wang[2,3], Xiaodong Liu[1], Yinan Zhang[2,3], Minakshi Bhardwaj[1], Anke Lemke[4], Daniel Wiegmann[4], Giuliana Niro[4], Jon S. Thorson[1,2], Christian Ducho[4] and Steven G. Van Lanen[1]✉

Several nucleoside antibiotics are structurally characterized by a 5″-amino-5″-deoxyribose (ADR) appended via a glycosidic bond to a high-carbon sugar nucleoside (5′*S*,6′*S*)-5′-*C*-glycyluridine (GlyU). GlyU is further modified with an *N*-alkylamine linker, the biosynthetic origin of which has yet to be established. By using a combination of feeding experiments with isotopically labeled precursors and characterization of recombinant proteins from multiple pathways, the biosynthetic mechanism for *N*-alkylamine installation for ADR-GlyU-containing nucleoside antibiotics has been uncovered. The data reveal *S*-adenosyl-L-methionine (AdoMet) as the direct precursor of the *N*-alkylamine, but, unlike conventional AdoMet- or decarboxylated AdoMet-dependent alkyltransferases, the reaction is catalyzed by a pyridoxal-5′-phosphate-dependent aminobutyryltransferase (ABTase) using a stepwise γ-replacement mechanism that couples γ-elimination of AdoMet with aza-γ-addition onto the disaccharide alkyl acceptor. In addition to using a conceptually different strategy for AdoMet-dependent alkylation, the newly discovered ABTases require a phosphorylated disaccharide alkyl acceptor, revealing a cryptic intermediate in the biosynthetic pathway.

Nucleoside antibiotics are a large family of natural products that have diverse biological activity and frequently complex structures requiring unparalleled biochemistry for their synthesis. Many nucleoside antibiotics inhibiting translocase I (TL1), involved in peptidoglycan synthesis, have recently been discovered[1] and several biochemical studies have already established numerous examples of the latter[2]. One group of TL1 inhibitors is structurally characterized by a disaccharide core consisting of an ADR linked to a high-carbon sugar nucleoside (GlyU), represented by FR-900493 (**1**), caprazamycin B (**2**), A-90289 B (**3**), sphaerimicin A (**4**), and muraymycin D1 (**5**) and D2 (**6**) (Fig. 1)[3–7]. The structures of **1**–**5** diverge outside of the shared ADR–GlyU disaccharide core, with each appended via a 6′-*N*-alkylamine linker to a unique glycosylated fatty acid, polyketide or peptide moiety. Compound 1, the structurally simplest of this nucleoside group with antibiotic activity, is modified with a methylated aminopropyl (C_3N) group attached to the ADR–GlyU disaccharide core. Structural inspection of **5** reveals the identical C_3N group, whereas **2** and **3** contain an aminobutyryl (C_4N) group that is further modified to a diazapenone ring.

The assembly of the ADR–GlyU disaccharide core has previously been delineated in vitro using the recombinant enzymes involved in the biosynthesis of **3** and **5** (refs. [8–11]). The pathway requires six enzymes that convert UMP and L-Thr to the ADR–GlyU disaccharide (see Supplementary Fig. 1a), and bioinformatic analysis suggests that these steps are shared for **2** and **4** (the gene cluster for **1** is unknown)[6,12]. However, the origin of the C_3N or C_4N units in these TL1 inhibitors, and the mechanism for their incorporation onto the ADR–GlyU disaccharide scaffold, has not been defined. Similar C_3N and C_4N units are found in several unrelated metabolites, for example various polyamines and siderophores, and they are known or hypothesized to be derived from either AdoMet or, less frequently, L-Asp-β-semialdehyde[13–15]. In the present study, we provide evidence to support a shared mechanism for the insertion of the C_3N group of **5** and the C_4N group of **3** which employs AdoMet as the direct metabolic precursor. Unlike other AdoMet-dependent alkylations, however, the process is highlighted by a fundamentally different catalytic strategy that involves γ-replacement by a pyridoxal-5′-phosphate (PLP)-dependent enzyme. Furthermore, the alkyl acceptor was unexpectedly determined to be the phosphorylated version of the ADR–GlyU disaccharide core, which was recently identified as the product of the kinase Mur28 from the biosynthetic pathway of **5** (ref. [16]). Although not readily apparent from the structure, the same alkylation strategy is also shown to initiate the biosynthesis of the highly unusual dihydroxylated piperidine ring of **4**.

Results

Metabolic origin of C_3N and C_4N units. The metabolic origin of the alkylamine linker was initially examined using feeding experiments with isotopically labeled precursors. *Streptomyces* species NRRL30475—a mutant strain of the native producer of muraymycins[7,16]—was chosen as the model system due to the reproducible and relatively acceptable titers of **5** (see Supplementary Note). Compound **5** contains a peptide that is predicted to be assembled by a nonribosomal peptide synthetase complex from L-Val, L-Arg, L-Leu and bicarbonate (see Supplementary Fig. 1b)[17]. Consequently, L-[1-^{13}C]Leu was fed as a positive control, and **5** was isolated and confirmed by ^{1}H-nuclear magnetic resonance (NMR) spectroscopy (see Supplementary Fig. 2a). High-resolution mass spectrometry (HR-MS) revealed that ~34% of **5** was enriched with a single ^{13}C atom (see Supplementary Fig. 3). Comparison of the ^{13}C-NMR spectra

[1]Department of Pharmaceutical Sciences, College of Pharmacy, University of Kentucky, Lexington, KY, USA. [2]Center for Pharmaceutical Research and Innovation, College of Pharmacy, University of Kentucky, Lexington, KY, USA. [3]Jiangsu Key Laboratory for Functional Substance of Chinese Medicine, School of Pharmacy, Nanjing University of Chinese Medicine, Nanjing, People's Republic of China. [4]Department of Pharmacy, Pharmaceutical and Medicinal Chemistry, Saarland University, Saarbrücken, Germany. ✉e-mail: svanlanen@uky.edu

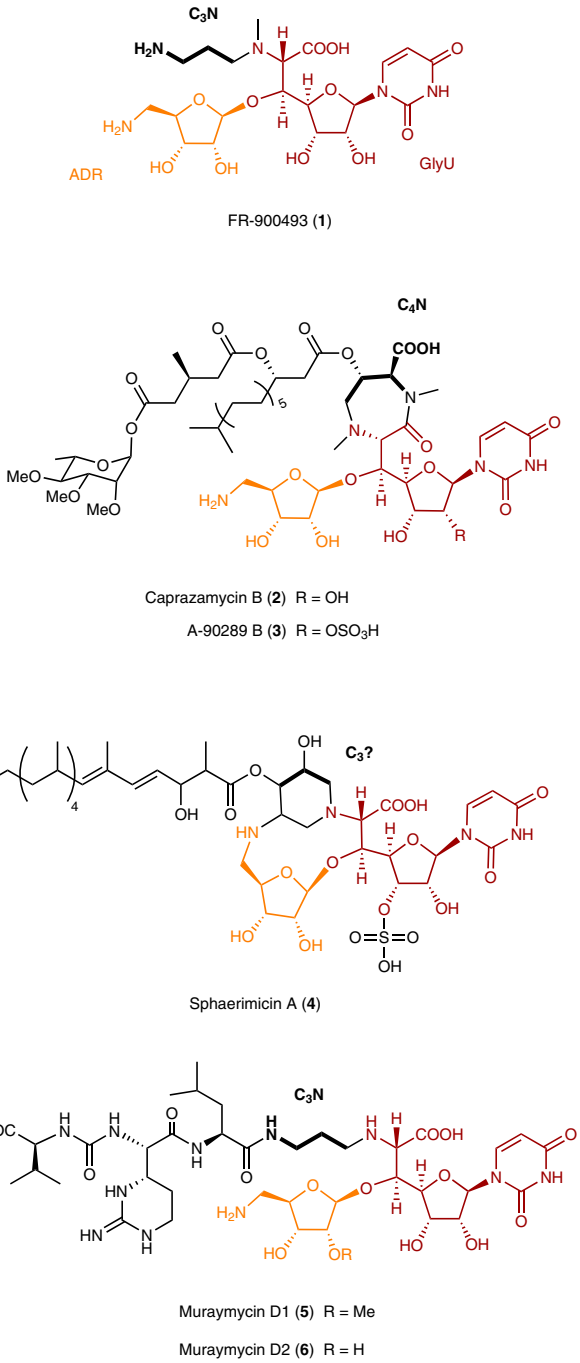

Fig. 1 | Structures of representative TL1 inhibitors that contain an *N*-alkylated ADR–GlyU disaccharide core. The *N*-alkylamine linker (C_3N or C_4N) of unknown biosynthetic origin connects structural components that are unique to each member.

revealed a clear enhancement of the 174.8 ppm signal that corresponds to the amide carbon of the Leu component, the expected site of incorporation (see Supplementary Fig. 2b). HR-MS/MS was likewise consistent with the regioselective incorporation of L-[1-^{13}C] Leu (see Supplementary Fig. 4). Subsequently, L-[$^{13}C_5$,^{15}N]Met, an established precursor of AdoMet, or L-[$^{13}C_4$,^{15}N]Asp, an established precursor of L-Asp-β-semialdehyde, was individually fed to the strain, and the isolation of **5** was confirmed by ^{1}H-NMR spectroscopy (see Supplementary Fig. 5). HR-MS analysis of **5** derived from the L-[$^{13}C_5$,^{15}N]Met feeding experiments revealed ~31% consisting of a +5-amu isotopologue (see Supplementary Fig. 6). Comparison of the ^{13}C-NMR spectra suggested no substantial enrichment when feeding L-[$^{13}C_4$,^{15}N]Asp, whereas an increase in the signal intensity of four peaks was observed when feeding L-[$^{13}C_5$,^{15}N]Met (Fig. 2). The peak signal at 58.0 ppm, previously assigned as the 2″-methyl ether, was enriched, which is consistent with alkylation catalyzed by an AdoMet-dependent *O*-methyltransferase. The remaining three signals at 45.6 (d), 25.0 (t) and 35.8 (dd) ppm—corresponding to C1‴–C3‴ of the aminopropyl linker of **5**, respectively—were similarly enriched, which is consistent with AdoMet as the direct precursor. HR-MS/MS further supported these findings (see Supplementary Fig. 7). The $^1J_{CC}$ splitting pattern and value (35.5 Hz) from L-[$^{13}C_5$,^{15}N]Met feeding suggested an intact incorporation of the C_3N unit. Importantly, the peak corresponding to C3‴ had a second coupling (7.8 Hz), which is consistent with expectations for $^1J_{CN}$ coupling in this chemical environment.

Aminobutyryltransferase functional assignment. C_3N and C_4N transferases with established functions have sequence and structural similarity to AdoMet-dependent methyltransferases[13–15,18–20]. The gene cluster for **5** encodes for a single protein (Mur11) with an AdoMet-dependent MTase domain. Homologous genes, however, are not found in the **2**–**4** biosynthetic gene cluster, and the gene product was tentatively assigned as the catalyst for 2″-*O*-methylation to convert **6** to 5. Armed with the knowledge that AdoMet or an L-Met-derived metabolite would ultimately need to undergo decarboxylation to generate **5**, similar to polyamine biosynthetic pathways that proceed through AdoMet decarboxylation before C_3N group transfer[13], the gene cluster for **5** was further analyzed for the presence of any remaining gene encoding a putative PLP-dependent decarboxylase. This search uncovered Mur23, which has a similarity to proteins annotated as diaminopimelate decarboxylases belonging to the conserved domain family of COG0019 (see Supplementary Fig. 8). A Mur23 homolog is not encoded in the **2** and **3** gene cluster, as expected, if Mur23 is indeed a decarboxylase. Another putative PLP-dependent protein, Mur24, with sequence similarity to proteins annotated as 1-aminocyclopropane-1-carboxylate (ACC) synthases, is encoded immediately downstream of *mur23*. The similarity of Mur24 to ACC synthases, which are PLP-dependent enzymes that use AdoMet to catalyze intramolecular C_α–C_γ bond formation, with concomitant C_γ–S bond cleavage to produce ACC and methylthioadenosine (MTA)[21], was intriguing due to the evidence that L-Met—probably by way of AdoMet—serves as the C_3N source of **5**. Phylogenetic analysis suggested that Mur24 occupies a separate clade, and hence might harbor a distinct activity, when compared with plant ACC synthases or the recently characterized bacterial ACC synthase, GnmY (see Supplementary Fig. 9)[22]. In contrast to *mur23*, genes homologous to *mur24* were identified within the **2** (*cpz13*) and **3** (*lipJ*) gene clusters, suggesting that this enzymatic step is shared in these pathways[12,23]. A gene (*sphL*) encoding a protein with sequence similarity to Mur24 was also identified within the **4** gene cluster[6]. The Mur24 homologs, which range from 34% to 50% in sequence identity using pairwise alignments, are part of the class I aminotransferase superfamily, and all retain a conserved Lys (corresponding to Lys 234 for Mur24 and Lys 229 for LipJ), which is predicted to be critical for PLP binding and enzymatic activity (see Supplementary Fig. 10).

Recombinant Mur24, purified to near homogeneity from *Streptomyces lividans* TK24 (see Supplementary Fig. 11), was initially screened for activity with two potential alkyl acceptors: (5′*S*,6′*S*)-GlyU (**7**), the demonstrated isomeric product of LipK and Mur17 involved in biosynthesis of **3** and **5**, respectively, and ADR–GlyU (**8**), the disaccharide product of the six-enzyme pathway that had been previously characterized (Fig. 3a)[9–11]. The acceptors were prepared by both chemical and chemoenzymatic synthesis, and the identity was confirmed by spectroscopic analyses

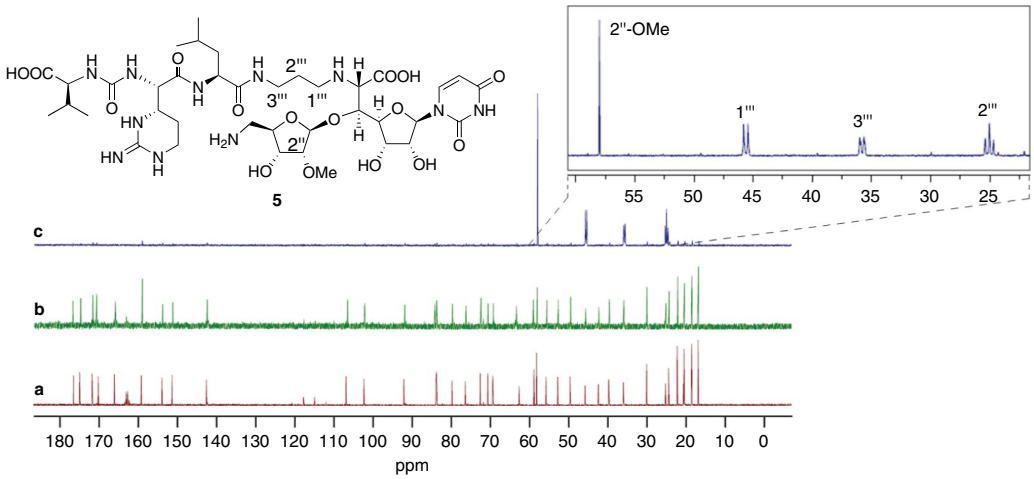

Fig. 2 | Spectroscopic analysis of feeding experiments. a–c, The ^{13}C-NMR spectrum (D_2O, 100 MHz) of **5** isolated without feeding (natural isotopic abundance; **a**), after feeding with L-[$^{13}C_4$,^{15}N]Asp (**b**) and after feeding with L-[$^{13}C_5$,^{15}N]Met (**c**). The inset of **c** depicts the zoomed-in region of the ^{13}C-NMR spectrum to emphasize the splitting pattern of the enriched carbons.

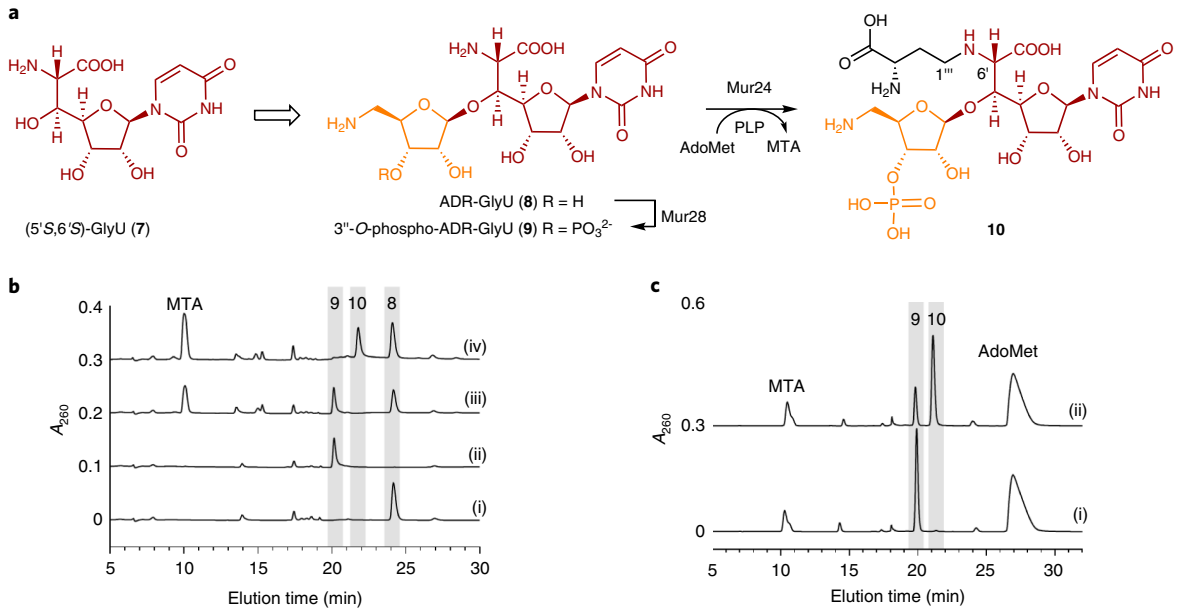

Fig. 3 | Functional assignment of Mur24. a, Structures of known products of enzyme reactions involved in the muraymycin biosynthetic pathway including the proposed reaction catalyzed by Mur24. **b**, HPLC traces of 6-h reactions catalyzed by Mur24 starting with ADR-GlyU (**8**) with the (i) exclusion of the phosphotransferase Mur28, (ii) reaction mixture containing ATP and Mur28, (iii) reaction mixture containing ATP, Mur28 and AdoMet with the exclusion of Mur24, and (iv) reaction mixture consisting of all the components. A_{260}, absorbance at 260 nm; a.u., arbitrary units. **c**, HPLC traces of reactions catalyzed by Mur24 starting from **9** with (i) reaction mixture with the exclusion of PLP and (ii) reaction mixture containing all components.

(see Supplementary Note). Based on the results from the isotopic enrichment experiments, L-Met, decarboxylated AdoMet (dcAdoMet) and AdoMet were tested as potential alkyl donors. Analysis of the reactions performed under a variety of conditions, including with or without exogenously supplied PLP, failed, however, to reveal a new peak. Reactions with recombinant LipJ and SphL (see Supplementary Fig. 11) also gave negative results.

Mur28 was previously shown to catalyze the phosphorylation of the 3″-OH of **6** and **8**, the latter generating 3″-*O*-phospho-**8** (**9**) (Fig. 3a). Single-substrate kinetic analysis revealed an approximately 60-fold higher catalytic efficiency with **8**, suggesting that phosphorylation occurs before the attachment of the C_3N-linked peptide component. Consequently, ATP and Mur28 were included in the Mur24 activity screen to generate **9** in situ as a potential alkyl acceptor for Mur24. HPLC analysis revealed the formation of a new peak that was dependent on the inclusion of AdoMet (Fig. 3b). MS analysis was consistent with Mur24-catalyzed alkylation of **9** to generate **10** (see Supplementary Note). Subsequently, **9** was enzymatically prepared and purified, and comparison of the MS and NMR spectra was consistent with 3″-OH as the site of phosphorylation as previously reported (see Supplementary Note)[16]. Using purified **9** as the alkyl acceptor, the identical result was obtained (Fig. 3c). HR-MS analysis of the product **10** yielded an $(M+H)^+$ ion at m/z=630.1643, which is consistent with the molecular formula for C_4N-modified-**9** (expected $(M+H)^+$ ion at m/z=630.1660 for $C_{20}H_{32}N_5O_{16}P$). Analysis by NMR spectroscopy (see Supplementary Note) further supported the structure of the Mur24 product **10** (Fig. 3a), and ^{1}H–^{13}C heteronuclear multiple bond coherence

correlations between C6′ of GlyU and C1‴ of the C_4N group supported the expected regiochemistry for C_4N attachment. The formation of **10** suggests that MTA is generated as the co-product, which was detected by HR-MS (see Supplementary Fig. 12). However, high background levels of MTA as a consequence of nonenzymatic AdoMet degradation precluded a quantitative assessment (Fig. 3). Overall, the data are consistent with the functional assignment of Mur24 as an AdoMet:**9** ABTase, generating **10** and probably MTA as co-products.

The activity of the Mur24 homologs LipJ and SphL, which are involved in the biosynthesis of **3** and **4**, respectively, was interrogated next. The gene cluster for **4** does not encode for a Mur28 phosphotransferase homolog, suggesting the possibility that phosphorylation of **8** is not a prerequisite for C_4N transfer by SphL. Conversely, the gene cluster for **3** encodes two Mur28 homologs, LipX (36% sequence identity) and LipI (23%), suggesting that LipJ has the same substrate specificity with respect to the alkyl acceptor as Mur24. Activity tests of LipJ with **9** and AdoMet revealed the formation of **10**, and the reaction was dependent on a phosphorylated acceptor as the substrate (see Supplementary Fig. 13a,b). Contrary to expectations, SphL catalyzed the same reaction wherein activity was strictly dependent on a phosphorylated acceptor **9** as the substrate (see Supplementary Fig. 13c), despite the absence of a phosphotransferase candidate. Overall the results establish the functional assignment of this group of proteins as AdoMet:**9** ABTases that catalyze γ-replacement of AdoMet, thereby breaking the Cγ–S bond while generating a new Cγ–N bond. Furthermore the results suggest that the biosynthesis of **3**–**5** occurs through **10**, an unexpected phosphorylated intermediate and probably the last shared intermediate of these pathways.

Biochemical characterization. After the functional assignment of the newly discovered ABTases, the biochemical properties were examined primarily using Mur24 as the model enzyme. When PLP was omitted from the reaction, a trace amount of **10** was detected (Fig. 3c). Subsequently, a Mur24(K234A) mutant was prepared, and the activity was abolished with or without the addition of PLP (see Supplementary Fig. 14). The same result was obtained with LipJ(K229A). Thus, the data are consistent with an important role for PLP in catalysis and that the Lys—predicted through bioinformatics analysis to form an internal aldimine with PLP—is essential (see Supplementary Fig. 10). Potential alternative alkyl donor substrates that are known to be (or hypothetically could be) derived from L-Met—including *S*-methylmethionine (SMM), ACC, 2-amino-3-butenoic acid (commonly referred to as L-vinylglycine (L-VG)), L-homoserine lactone and the AdoMet analog sinefungin (see Supplementary Fig. 15a)—were next tested with Mur24. Cystathionine and *O*-succinyl-L-homoserine were also screened as potential C_4N donors. Only SMM, an abundant plant metabolite that can be metabolized by some animals and bacteria[24], could substitute for AdoMet as an alkyl donor (see Supplementary Fig. 15b). The relative activity with SMM was substantially reduced (9% yield of **10** relative to AdoMet), suggesting that AdoMet is the substrate in vivo. Using precolumn modification with 3-methyl-2-benzothiazolinone hydrazine hydrochloride (MBTH), a relatively minor amount of L-VG was converted to α-ketobutyrate (αKB) and NH_3 by Mur24. Time-course analysis gave a specific activity of 0.05 min^{-1} for this reaction (see Supplementary Fig. 15c), a 54-fold reduction compared with the calculated turnover for the alkyl transfer reaction with AdoMet. Thus, similar to ACC synthase, L-VG serves as an alternative but inferior substrate for an aminotransferase side reaction[21]. However, incubation of L-VG with Mur24 and **9** under a variety of reaction conditions did not yield detectable **10**. This result is in contrast to that observed with cystathionine γ-synthase (CSG synthase), which catalyzes γ-replacement of the α-amino acid *O*-succinyl-L-homoserine with the sulfhydryl group of L-Cys to generate L-cystathionine and succinate (see Supplementary Fig. 16a), and can catalyze γ-addition starting with L-VG and L-Cys at pH 8.3 (ref. [25]). Finally, the *(S)*- and *(R)*-sulfonium isomers of commercial AdoMet, the former being the biologically relevant diastereomer generated by AdoMet synthetase (MAT), were separated by HPLC and tested with Mur24 (see Supplementary Fig. 17a). Unexpectedly, both isomers were functional as alkyl donors to convert **9** to **10** (see Supplementary Fig. 17b).

The same panel of hypothetical alkyl donors was also tested for inhibition of the Mur24-catalyzed reaction using conditions promoting an almost-complete conversion of **9** to **10** with AdoMet as the alkyl group donor. SMM, which undergoes trace turnover when substituting for AdoMet under these conditions, inhibited the reaction at a 2:1 molar ratio relative to AdoMet (see Supplementary Fig. 18a). Sinefungin, a well-known inhibitor of many AdoMet-dependent methyltransferases, likewise inhibited the Mur24-catalyzed formation of **10** using either AdoMet or SMM as the alkyl donor (see Supplementary Fig. 18a). The remaining L-Met analogs including L-VG, which is an established mechanism-based inhibitor of ACC synthase[26,27], had no effect on the production of **10** (see Supplementary Fig. 18b). Similarly, the addition of ethylenediaminetetraacetic acid, Zn^{2+} or sulfhydryl-modifying reagents had no effect. Finally, by directly detecting the formation of **10** by HPLC, single-substrate kinetic analysis revealed Michaelis–Menten kinetics with respect to varied **9** (see Supplementary Fig. 19), yielding a Michaelis constant, $K_m = 92 \pm 8\,\mu M$, and catalytic constant, $k_{cat} = 2.7 \pm 0.2\,min^{-1}$. The limiting amount of available **9** precluded an accurate assessment of the kinetic parameters for co-substrate AdoMet.

Mechanistic insight. Enzymatic alkyl group transfer from AdoMet to a nitrogen nucleophile of an acceptor substrate is generally considered to occur by S_N2 nucleophilic substitution. However, the PLP dependency of these newly discovered ABTases suggests that γ-replacement with AdoMet occurs through a stepwise γ-elimination–γ-addition similar to CSG synthase[25,28–30]. Mechanistic insight for PLP-dependent enzymes such as CSG synthase can often be garnered by monitoring PLP-bound intermediates by ultraviolet–visible (UV/Vis) spectroscopy[28]; however, spectral snapshots of the Mur24 reaction under steady-state conditions provided marginal information on the mechanism and role of PLP (see Supplementary Fig. 20). We therefore opted to track the hydrogen atoms before and after C_4N group transfer as a way of discriminating between mechanistic possibilities. Three AdoMet isotopologues were prepared in situ using differentially deuterated L-Met and human MAT isoform 2A (hMAT2A) (Fig. 4). Starting with L-[2,3,3,4,4-$^2H_5$;*methyl*-$^2H_3$]Met and monitoring the Mur24-catalyzed formation of **10** by HR-MS, an $(M+H)^+$ ion at $m/z = 633.1835$ was detected (expected $(M+H)^+$ ion at $m/z = 633.1848$ for $C_{20}H_{29}D_3N_5O_{16}P$), consistent with the retention of three of eight deuterium atoms when compared with unlabeled L-Met control (detected $m/z = 630.1615$). An $(M+H)^+$ ion at $m/z = 633.1859$ was observed with L-[2,3,3,4,4-$^2H_5$]Met, again indicating the retention of three deuterium atoms. Finally, an $(M+H)^+$ ion at $m/z = 630.1653$ was detected when starting with L-[2-^2H]Met, revealing the loss of the single deuterium during the formation of **10**.

Reactions starting with **9** and natural abundance AdoMet were performed in D_2O, and isotopic distribution revealed that most of **10** was monodeuterated (60%) with some dideuterated (19%) after 6 h (see Supplementary Fig. 21a). The potential reversibility of the Mur24-catalyzed reaction was also examined. Although no products were observed when starting with **10** and MTA, time-course analysis of reactions in D_2O revealed a relatively fast incorporation of one deuterium into **10** (specific activity of $1.2\,\mu mol\,min^{-1}\,mg^{-1} \approx 62\,min^{-1}$) and a slow formation of dideuterated **10** ($2.0 \times 10^{-2}\,\mu mol\,min^{-1}\,mg^{-1} \approx 1.0\,min^{-1}$; see Supplementary Fig. 21b,c). After a 6-h reaction, isotopic distribution revealed that

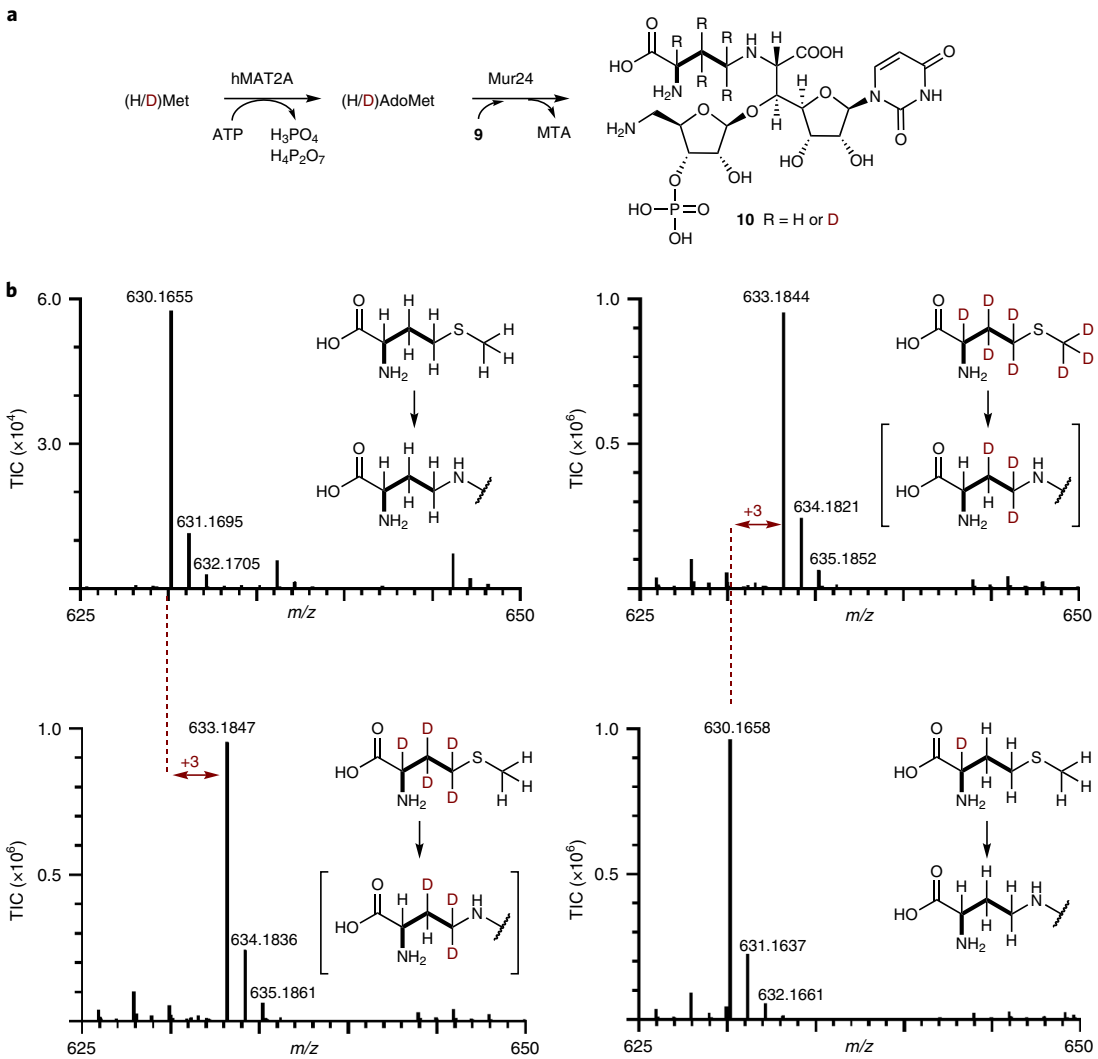

Fig. 4 | Isotopic incorporation from L-Met. a, Enzymatic scheme starting with differentially deuterated L-Met for generating AdoMet isotopologues as a substrate for Mur24. **b**, HR-MS data for **10** starting with the indicated L-Met isotopologue. TIC, total ion count. The regiochemistry of the incorporated deuteriums in the bracketed products is proposed.

most of **10** was monodeuterated (75%) with some dideuterated (9%). Overall, the data are consistent with two exchangeable hydrogen atoms from AdoMet—one bonded to C_2 and the other to C_3 or C_4—during the C_4N group transfer reaction.

Enzymatic decarboxylation of 10. The functional assignment of the PLP-dependent ABTases suggested that, unlike classic AdoMet-dependent polyamine biosynthesis, decarboxylation during biosynthesis of **5** occurs after transfer of an alkyl group. To explore this possibility, recombinant Mur23 was produced and purified (see Supplementary Fig. 11d). Unlike the ABTases, Mur23 co-purified with PLP, as evident from the yellow color and the characteristic UV/Vis spectrum (see Supplementary Fig. 22). LC–MS analysis of reactions of Mur23 with **10** yielded a new peak (Fig. 5), with an $(M+H)^+$ ion at $m/z = 586.1748$, consistent with the molecular formula for decarboxylated **10** (**11**) (expected $(M+H)^+$ ion at $m/z = 586.1756$ for $C_{19}H_{32}N_5O_{14}P$) (see Supplementary Note). The structure of **11** was further supported by MS and NMR spectroscopy (see Supplementary Note). In contrast to reactions with **10**, Mur23 was unable to catalyze decarboxylation of AdoMet or dephospho-**10** (**12**) (see Supplementary Fig. 23), the latter generated by reacting **10** with calf intestinal phosphatase and confirmed by MS (see Supplementary Note). Single-substrate kinetic analysis revealed Michaelis–Menten kinetics with respect to varied **10** (see Supplementary Fig. 19b), yielding a $K_m = 701.8 \pm 9.2\,\mu M$ and $k_{cat} = 144.8 \pm 1.1\,min^{-1}$, equating to an apparent second-order rate constant $k_{cat}/K_m \sim 3.3 \times 10^3\,M^{-1}\,s^{-1}$, a sixfold greater catalytic efficiency compared with Mur24 ($k_{cat}/K_m \approx 5 \times 10^2\,M^{-1}\,s^{-1}$). The K_m value for Mur23, although relatively high, is within the range observed for other PLP-dependent decarboxylases (see Supplementary Fig. 8). Overall the data support the functional assignment of Mur23 as a **10** decarboxylase (Fig. 5b).

Discussion

AdoMet is perhaps best known as a methyl donor, although this ubiquitous metabolite also serves as the source of C_3N and C_4N alkyl groups in the biosynthesis of many structurally distinct metabolites. For C_3N group biosynthesis, a PLP-dependent decarboxylase first generates dcAdoMet, which serves as the substrate for a distinct alkyltransferase that catalyzes C_3N group transfer independent of cofactors. These C_3N alkyltransferases have structural similarity to AdoMet-dependent methyltransferases, and consequently have been proposed as originating via divergent evolution. AdoMet, as a C_4N group donor, has likewise been noted in several metabolic

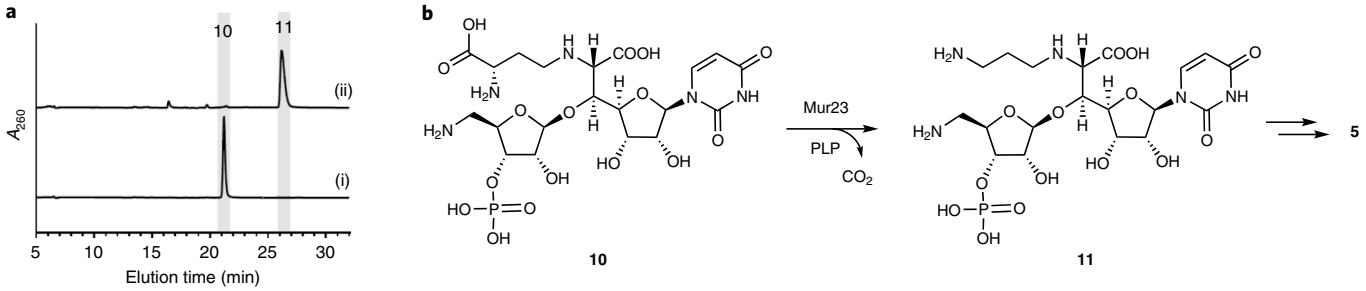

Fig. 5 | Functional assignment of Mur23. a, HPLC traces of (i) control without enzyme and (ii) reaction catalyzed by Mur23 starting from **10** and PLP. A_{260}, absorbance at 260 nm. **b**, Chemical reaction catalyzed by Mur23.

pathways[14,20,31–34]. Similar to the C_3N alkyltransferases, the available data suggest the C_4N alkyltransferases are also structurally, mechanistically and evolutionarily related to methyltransferases[18,19]. The data in the present article have provided evidence of a C_4N alkyl group transfer from AdoMet by a new family of enzymes most closely related to plant PLP-dependent ACC synthases[26,35].

Canonical AdoMet- or dcAdoMet-dependent alkyl group transfer is generally believed to occur by an S_N2 substitution, wherein the nucleophile directly attacks the carbon adjacent to the sulfonium. Consequently, no exchange of carbon-bonded hydrogen atoms would be expected during the reaction. Similarly, the ACC synthase reaction proceeds without exchange[21]. The results with Mur24 revealed two exchangeable hydrogen atoms, which is consistent with alkyl group transfer from AdoMet via a stepwise reaction proceeding through sequential γ-elimination (lyase) and aza-Michael γ-addition (synthase) chemistry. Although less-favored mechanisms remain possible, we propose the following mechanism that is comparable to the γ-replacement mechanism put forth for CSG synthase (Fig. 6)[28–30,36]. PLP and AdoMet first generate an external aldimine I that is commonplace for PLP-dependent enzymes. Interestingly, unlike many PLP-dependent enzymes, including CSG synthase[28], the recombinant ABTases do not co-purify with PLP under a variety of conditions screened. After the formation of a pseudo-Michaelis (ternary) complex, a general base—probably Lys 234 for Mur24—abstracts the C_α proton. This step, again well established for many PLP-dependent enzymes, is supported by the deuterium-labeling experiments. Due to the lack of a diagnostic absorption band for a quinonoid (see Supplementary Fig. 20), C_α deprotonation is probably immediately followed by C4′ protonation, generating the ketimine II. Subsequently, the C_β proton—rendered relatively more acidic due to the vicinal iminium—is abstracted to form the enamine III before formation of a transient β,γ-unsaturated ketimine IV with concomitant elimination of MTA. The intermediacy of enamine III is supported by the deuterium 'wash-in' experiments with **10**, which demonstrate Mur24-catalyzed exchange of the α and β hydrogens without γ-elimination. In the presence of **9**, that is the true Michaelis complex, the amine nucleophile is deprotonated by an unidentified general base and attacks C_γ in an aza-Michael-type nucleophilic addition, and the reverse of the previous steps affords **10**.

Potentially the most intriguing feature of the Mur24-catalyzed reaction is the chemical functionality involved in the bond-breaking and bond-making steps to transform one γ-substituted, α-amino acid to another. CSG synthase and *O*-acetyl-L-homoserine sulfhydrylase[37], enzymes catalyzing a native PLP-dependent γ-replacement, initiate their reactions by breaking a C_γ–OC(O)R bond before the formation of a new C_γ–S bond (see Supplementary Fig. 16a). These enzymes, along with two other PLP-dependent enzymes, L-Met γ-lyase and cystathionine γ-lyase, have been shown to catalyze reactions in vitro using nucleophiles other than thiols, including selenium/selenols (Cγ–Se) and cyanide (Cγ–C), although the biological relevance of these reactions is unknown (see Supplementary Fig. 16b)[38–41]. Mur24 and homologous ABTases clearly differ from these γ-replacement enzymes by using a sulfonium substrate, thereby breaking a Cγ–S^+ bond, and using a primary amine of an amino acid acceptor, thereby generating a Cγ–N bond. This aza-Michael-type 1,4-addition, a comparable second half-reaction of which has been proposed during ergot alkaloid biosynthesis, but for which the putative enzyme catalyst has not yet been characterized (see Supplementary Fig. 16c)[42], is a considerable chemical feat. The general interest in having mild and simple methodologies to introduce unfunctionalized C–N bonds via aza-Michael additions has resulted in multiple reports detailing new synthetic catalysts and strategies[43,44]. Consequently, a few enzymes have been discovered to catalyze an aza-Michael-type γ-addition that is similar to the addition half-reaction addressed here, although an entirely different, PLP-independent, catalytic strategy is used to afford a new C–N bond[45,46]. Interestingly, an enzyme, SbnA, involved in the biosynthesis of L-2,3-diaminopropionic acid, has recently been shown to catalyze a PLP-dependent, β-replacement reaction using the amine of L-Glu as a nucleophile for addition[47]. However, the reaction involves a β-replacement as opposed to the γ-replacement, a fundamental difference between the two enzymes. The catalytic strategy used by Mur24 and SbnA to activate amine nucleophiles for γ- and β-addition reactions, respectively, and how this compares with other β- and γ-replacement enzyme catalysts, can now be addressed.

CSG synthase catalyzes a well-characterized, γ-replacement reaction with a specific activity of 100 μmol min^{-1} mg^{-1} (~240 min^{-1})[30]. CSG synthase can also convert L-VG and L-Cys to cystathionine, thereby bypassing the first half (that is, γ-elimination) reaction[25]. The newly discovered ABTases cannot bypass the elimination step by using L-VG as an alkyl donor. The ability of CSG synthase to use L-VG directly for γ-addition has been speculated to be due to solvent accessibility to the active site[25], which compensates for the incorrect protonation state of the general base/acid ($EnzB_1$ in Fig. 6) responsible for C_β deprotonation (during γ-elimination) and re-protonation (during γ-addition). Using cystathionine, CSG synthase catalyzes isotope exchange from ^3H_2O to both C_α and C_β protons—with a twofold preference for C_β exchange over C_α—at rates more than sevenfold faster than the overall γ-replacement reaction[30]. Mur24 can catalyze a similar isotope exchange from D_2O to **9** that is comparably faster (~23-fold) than γ-replacement. However, the data establish a strong preference for the exchange of a single hydrogen per molecule instead of two (62-fold difference), suggesting that one site, which we propose is C_β, is better shielded from bulk solvent and hence cannot support γ-addition starting with L-VG. The differences in reactivity of CSG synthase and the ABTases could also be the result of the nature of the acceptor nucleophile. Thiols/thiolates, for example the L-Cys acceptor for CSG synthase, are excellent nucleophiles for conjugate additions, and the softness enables orbital effects to dominate the reaction with the relatively soft electrophilic center at C_γ (refs. [48,49]). The PLP-dependent ABTases use a relatively hard amine nucleophile,

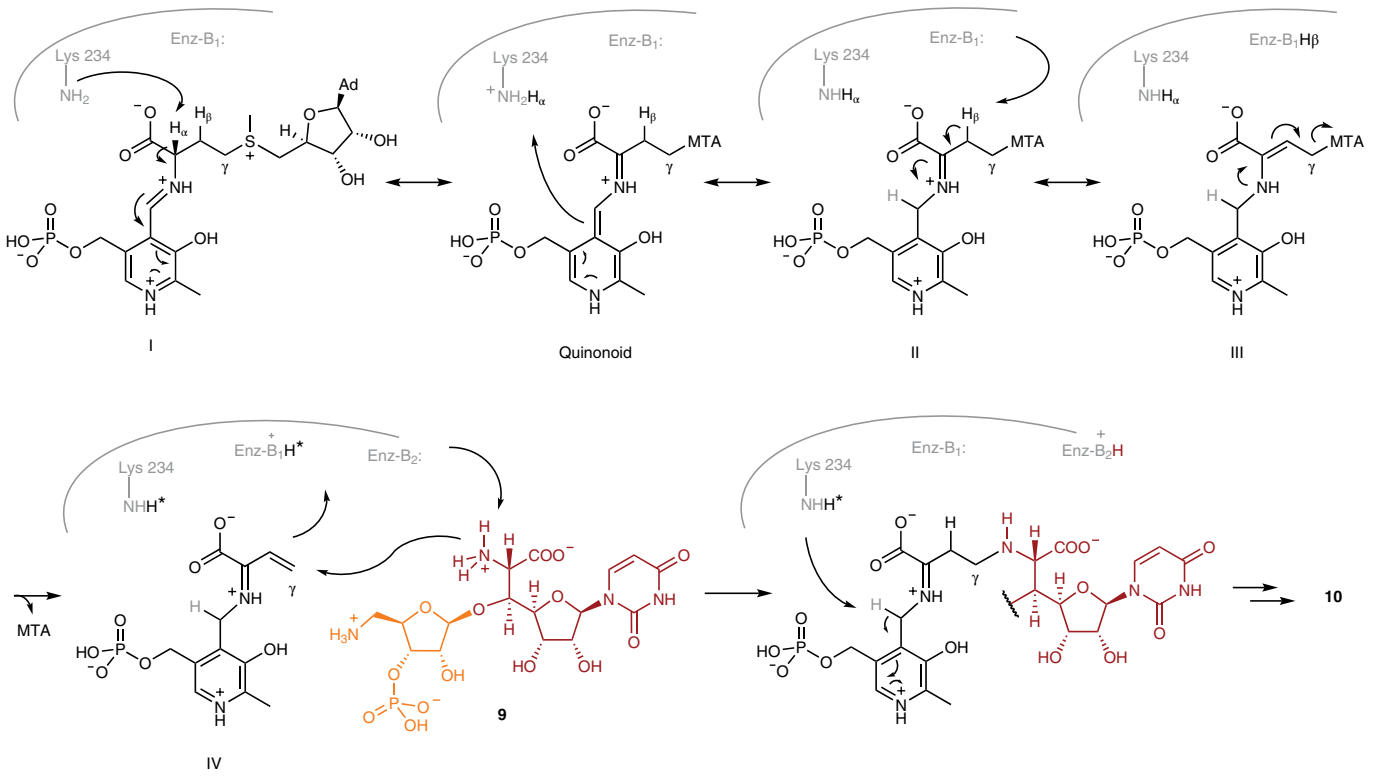

Fig. 6 | Putative γ-elimination and γ-addition mechanism for the PLP-dependent AdoMet:9 ABTases. The asterisk indicates a proton that differs from the H_β that is removed from the substrate, which is consistent with isotopic labeling. After the formation of ketimine II, deprotonation at C_β could hypothetically generate an enamine (C_α–C_β double bond), which is not shown, before γ-elimination to generate the β,γ-unsaturated ketimine III.

thereby relying more on charges and electrostatic effects to catalyze conjugate γ-addition. Consequently, the correct protonation state is probably critical for PLP-dependent ABTase activity, and this can be achieved only on catalyzing γ-elimination of the substrate. Ongoing structural and biochemical studies will undoubtedly help clarify the observed differences in the chemistry.

Finally, the discovery of the PLP-dependent C_4N alkyltransferases has revealed that the biosynthetic pathway for **3**–**5** proceeds through a cryptic phosphorylated intermediate. This discovery is consistent with the isolation of a phosphorylated caprazol from a mutant strain of the **2** producer[50], as well as the previous functional assignment of the kinase Mur28 involved in biosynthesis of **5** (ref. [16]). The results establish **10** as the most probable last shared intermediate, on which the pathways diverge to afford the structurally unique scaffolds of **1**–**5**. Pathway divergence for **5** is initiated by Mur23-catalyzed **10** decarboxylation which, when combined with the preceding Mur24-catalyzed alkyl transfer, has revealed a new, 'inverse', polyamine biosynthetic strategy using two consecutive PLP-dependent enzymes to incorporate an aminopropyl linker derived from the exceptionally versatile metabolite AdoMet.

Statistics and reproducibility. HPLC traces and MS spectra are representative of data collected minimally twice independently with similar results. Data points in scatter plots represent the average of three independent experiments unless noted in the figure legend, and the error bars depict the s.d.

Online content

Any Nature Research reporting summaries, source data, supplementary information, acknowledgements, peer review information; details of author contributions and competing interests; and statements of data and code availability are available at https://doi.org/10.1038/s41589-020-0548-3.

Received: 1 November 2019; Accepted: 10 April 2020;
Published online: 01 June 2020

References

1. Winn, M., Goss, R. J., Kimura, K. & Bugg, T. D. Antimicrobial nucleoside antibiotics targeting cell wall assembly: recent advances in structure–function studies and nucleoside biosynthesis. *Nat. Prod. Rep.* **27**, 279–304 (2010).
2. Shiraishi, T. & Kuzuyama, T. Recent advances in the biosynthesis of nucleoside antibiotics. *J. Antibiot.* **72**, 913–923 (2019).
3. Hirano, S., Ichikawa, S. & Matsuda, A. Total synthesis of (+)-FR-900493 and establishment of its absolute stereochemistry. *Tetrahedron* **63**, 2798–2804 (2007).
4. Igarashi, M. et al. Caprazamycins, novel lipo-nucleoside antibiotics, from *Streptomyces* sp. II. Structure elucidation of caprazamycins. *J. Antibiot.* **58**, 327–337 (2005).
5. Fujita, Y. et al. A-90289 A and B, new inhibitors of bacterial translocase I, produced by *Streptomyces* sp. SANK 60405. *J. Antibiot.* **64**, 495–501 (2011).
6. Funabashi, M. et al. Structure-based gene targeting discovery of sphaerimicin, a bacterial translocase I inhibitor. *Angew. Chem. Int. Ed.* **52**, 11607–11611 (2013).
7. McDonald, L. A. et al. Structures of the muraymycins, novel peptidoglycan biosynthesis inhibitors. *J. Am. Chem. Soc.* **124**, 10260–10261 (2002).
8. Yang, Z. et al. Characterization of LipL as a non-heme, Fe(II)-dependent α-ketoglutarate:UMP dioxygenase that generates uridine-5′-aldehyde during A-90289 biosynthesis. *J. Biol. Chem.* **286**, 7885–7892 (2011).
9. Barnard-Britson, S. et al. Amalgation of nucleosides and amino acids in antibiotic biosynthesis: discovery of an L-threonine:uridine-5′-aldehyde transaldolase. *J. Am. Chem. Soc.* **134**, 18514–18517 (2012).
10. Chi, X., Pahari, P., Nonaka, K. & Van Lanen, S. G. Biosynthetic origin and mechanism of formation of the aminoribosyl moiety of peptidyl nucleoside antibiotics. *J. Am. Chem. Soc.* **133**, 14452–14459 (2011).
11. Cui, Z. et al. Enzymatic synthesis of the ribosylated glycyl-uridine disaccharide core of peptidyl nucleoside antibiotics. *J. Org. Chem.* **83**, 7239–7249 (2018).
12. Kaysser, L. et al. Identification and manipulation of the caprazamycin gene cluster lead to new simplified liponucleoside antibiotics and give insights into the biosynthetic pathway. *J. Biol. Chem.* **284**, 14987–14996 (2009).
13. Michael, A. J. Biosynthesis of polyamines and polyamine-containing molecules. *Biochem. J.* **473**, 2315–2329 (2016).

14. Dreyfus, C., Lemaire, D., Mari, S., Pignol, D. & Arnoux, P. Crystallographic snapshots of iterative substrate translocations during nicotianamine synthesis in archaea. *Proc. Natl. Acad. Sci. USA* **106**, 16180–16184 (2009).
15. Lee, J. et al. An alternative polyamine biosynthetic pathway is widespread in bacteria and essential for biofilm formation in *Vibrio cholera*. *J. Biol. Chem.* **284**, 9899–9907 (2009).
16. Cui, Z. et al. Self-resistance during muraymycin biosynthesis: a complementary nucleotidyltransferase and phosphotransferase with identical modification sites and distinct temporal order. *Antimicrob. Agents Chemother.* **62**, e00193-18 (2018).
17. Cheng, L. et al. Identification of the gene cluster involved in muraymycin biosynthesis from *Streptomyces* sp. NRRL 30471. *Mol. Biosyst.* **7**, 920–927 (2011).
18. Ikeguchi, Y., Bewley, M. C. & Pegg, A. E. Aminopropyltransferases: function, structure, and genetics. *J. Biochem.* **139**, 1–9 (2006).
19. Martin, J. L. & McMillan, F. M. SAM (dependent) I AM: the *S*-adenosylmethioine-dependent methyltransferase fold. *Curr. Opin. Struct. Biol.* **12**, 783–793 (2002).
20. Reeve, A. M., Breazeale, S. D. & Townsend, C. A. Purification, characterization, and cloning of an *S*-adenosylmethionine-dependent 3-amino-3-carboxypropyltransferase in nocardicin biosynthesis. *J. Biol. Chem.* **1998**, 30695–30703 (1998).
21. Ramalingam, K., Lee, K.-M., Woodard, R. W., Bleecker, A. B. & Kende, H. Stereochemical course of the reaction catalyzed by the pyridoxal phosphate-dependent enzyme 1-aminocyclopropane-1-carboxylate synthase. *Proc. Natl. Acad. Sci. USA* **82**, 7820–7824 (1985).
22. Xu, Z., Pan, G., Zhou, H. & Shen, B. Discovery and characterization of 1-aminocyclopropane-1-carboxylic acid synthase of bacterial origin. *J. Am. Chem. Soc.* **149**, 16957–16961 (2018).
23. Funabashi, M. et al. The biosynthesis of liposidomycin-like A-90289 antibiotics featuring a new type of sulfotransferase. *ChemBioChem* **11**, 184–190 (2010).
24. Ko, S., Eliot, A. C. & Kirsch, J. F. *S*-Methylmethionine is both a substrate and an activator of 1-aminocyclopropane-1-carboxylate synthase. *Arch. Biochem. Biophys.* **42**, 85–90 (2004).
25. Johnston, M., Marcotte, P., Donovan, J. & Walsh, C. Mechanistic studies with vinylglycine and β-haoloaminobutyrates as substrates for cystathionine γ-synthase from *Salmonella typhimurium*. *Biochemistry* **18**, 1729–1738 (1979).
26. Feng, L. & Kirsch, J. F. L-Vinylglycine is an alternative substrate as well as mechanism-based inhibitor of 1-aminocyclopropane-1-carboxylate synthase. *Biochemistry* **39**, 2436–2444 (2000).
27. Capitani, G., Tschopp, M., Eliot, A. C., Kirsch, J. F. & Grütter, M. G. Structure of ACC synthase inactivated by the mechanism-based inhibitor L-vinylglycine. *FEBS Lett.* **579**, 2458–2462 (2005).
28. Guggenheim, S. & Flavin, M. Cystathionine γ-synthase from *Salmonella*. Spectral changes in the presence of substrates. *J. Biol. Chem.* **246**, 3562–3568 (1971).
29. Chang, M. N. T. & Walsh, C. T. Stereochemical analysis of γ-replacement and γ-elimination processes catalyzed by a pyridoxal phosphate enzyme. *J. Am. Chem. Soc.* **103**, 4921–4927 (1981).
30. Guggenheim, S. & Flavin, M. Cystathionine γ-synthase. A pyridoxal enzyme catalyzing rapid exchange of β and α hydrogen atoms in amino acids. *J. Biol. Chem.* **244**, 6217–6227 (1969).
31. Krog, J. S. et al. 3-(3-amino-3-carboxypropyl)-5,6-dihydrouridine is one of two novel post-transcriptional modifications in tRNALys(UUU) from *Trypanosoma brucei*. *FEBS J.* **278**, 4782–4796 (2011).
32. Nishimura, S., Taya, Y., Kuchino, Y. & Oashi, Z. Enzymatic synthesis of 3-(3-amino-3-carboxypropyl)uridine in *Escherichia coli* phenylalanine transfer RNA: transfer of the 3-amino-acid-3-carboxypropyl group from *S*-adenosylmethionine. *Biochem. Biophys. Res. Commun.* **57**, 702–708 (1974).
33. Ikegami, F. et al. Biosynthesis in vitro of 2-(3-amino-3-carboxypropyl)-isoxazolin-5-one, the neurotoxic amino acid in *Lathyrus odoratus*. *Biol. Pharm. Bull.* **16**, 732–734 (1993).
34. Taya, Y., Tanaka, Y. & Nishimura, S. Cell-free biosynthesis of discadenine, a spore germination inhibitor of *Dictyostelium discoideum*. *FEBS Lett.* **89**, 326–328 (1978).
35. Schneider, G., Käck, H. & Lindqvist, Y. The manifold of vitamin B_6 dependent enzymes. *Structure* **8**, R1–R6 (2000).
36. Brzović, P., Litzenberger Holbrook, E., Greene, R. C. & Dun, M. F. Reaction mechanism of *Escherichia coli* cystathionine γ-synthase: direct evidence for a pyridoxamine derivative of vinylglyoxylate as a key intermediate in pyridoxal phosphate dependent γ-elimination and γ-replacement reaction. *Biochemistry* **29**, 442–451 (1990).
37. Yamagata, S. Roles of *O*-acetyl-L-homoserine sulfhydrylases in microorganisms. *Biochimie* **71**, 1125–1143 (1989).
38. Esaki, N., Tanaka, H., Uemuru, S., Suzuki, T. & Soda, K. Catalytic action of L-methionine γ-lyase on selenomethionine and selenols. *Biochemistry* **18**, 407–410 (1979).
39. Sato, D. & Nozaki, T. Methionine gamma-lyase: the unique reaction mechanism, physiological roles, and therapeutic applications against infectious diseases and cancers. *IUBMB Life* **61**, 1019–1028 (2009).
40. Omura, H. et al. Purification, characterization and gene cloning of thermostable *O*-acetyl-L-homoserine sulfhydrylase forming γ-cyano-α-aminobutyric acid. *J. Biosci. Bioeng.* **96**, 53–58 (2003).
41. Chiku, T. et al. H_2S biogenesis by human cystathionine γ-lyase leads to the novel sulfur metabolites lanthionine and homolanthionine and is responsive to the grade of hyperhomocysteinemia. *J. Biol. Chem.* **284**, 11601–11612 (2009).
42. Faulkner, J. R. et al. On the sequence of bond formation in loline alkaloid biosynthesis. *ChemBioChem* **7**, 1078–1088 (2006).
43. Enders, D., Wang, C. & Liebich, J. X. Organocatalytic aza-Michael additions. *Chem. Eur. J.* **15**, 11058–11076 (2009).
44. Freedy, A. M. et al. Chemoselective installation of amine bonds on proteins through aza-Michael ligation. *J. Am. Chem. Soc.* **139**, 18365–18375 (2017).
45. Xu, F., Wu, Q., Chen, X., Lin, X. & Wu, Q. A single lipase-catalysed one-pot protocol combining aminolysis resolution and aza-Michael addition: an easy and efficient way to synthesise β-amino acid esters. *Eur. J. Org. Chem.* **2015**, 5393–5401 (2015).
46. Chisuga, T., Miyanaga, A., Kudo, F. & Eguchi, T. Structural analysis of the dual-function thioesterase SAV606 unravels the mechanism of Michael addition of glycine to an α,β-unsaturated thioester. *J. Biol. Chem.* **292**, 10926–10937 (2017).
47. Kobylarz, M. J. et al. Deciphering the substrate specificity of SbnA, the enzyme catalyzing the first step in staphyloferrin B biosynthesis. *Biochemistry* **55**, 927–939 (2016).
48. Brotzel, F. & Mayr, H. Nucleophilicities of amino acids and peptides. *Org. Biomol. Chem.* **5**, 3814–3820 (2007).
49. Clayden, J., Greeves, N. & Warren, S. *Organic Chemistry*, 2nd edn (Oxford University Press, 2012).
50. Shiraishi, T., Hiro, N., Igarashi, M., Nishiyama, M. & Kuzuyama, T. Biosynthesis of the antituberculosis agent caprazamycin: identification of caprazol-3″-phosphate, an unprecedented caprazamycin-related metabolite. *J. Gen. Appl. Microbiol.* **62**, 164–166 (2016).

Methods

Chemicals, bacterial strains and instrumentation. Chemicals and solvents were purchased from standard sources: L-[2,3,3,4,4-$^2H_5$;*methyl*-$^2H_3$]Met, L-[2,3,3,4,4-$^2H_5$]Met and L-[2-^2H]Met were purchased from CDN isotopes. An (*S*)- and (*R*)-AdoMet mixture (~3:2) was purchased from Santa Cruz Biotechnology. Compounds **7** and **8** were prepared as described (see Supplementary Note)[16,51,52]. Synthetic oligonucleotides were purchased from Integrated DNA Technologies. Phusion DNA polymerase, restriction enzymes and T4 DNA ligase were obtained from New England Biolabs Inc. and used according to the manufacturer's instructions. LA-Taq polymerase was obtained from Takara Bio Inc. DNA sequencing was carried out by ACGT Inc. The muraymycin-producing strains *Streptomyces* spp. NRRL30475 and NRRL30473 were obtained from the ARS Culture Collection (NRRL). *Escherichia coli* NEB5α, *E. coli* BL21(DE3) and *S. lividans* TK24 were used for routine cloning and protein expression.

NMR data were recorded at 400 MHz for ^1H and 100 MHz for ^{13}C using a Varian Inova NMR spectrometer or 600 MHz for ^1H and 150 MHz for ^{13}C using an Agilent 600/54 NMR spectrometer. HPLC analysis was performed on an Agilent 1200 system equipped with a photodiode array detector and an analytical SeQuant ZIC-HILIC column (5 µm, 200 Å (20 nm), 250 mm × 4.6 mm), an Alltech Apollo C18 column (5 µm, 100 Å, 250 mm × 4.6 mm) or a Thermo Scientific Acclaim 120 C18 column (5 µm, 120 Å, 100 mm × 4.6 mm). Semi-preparative HPLC was performed on a Waters 600 equipped with a photodiode array detector and an Alltech Apollo C18 column (5 µm, 100 Å, 250 mm × 10 mm). LC–MS was conducted using an Agilent 6120 Quadrupole MSD mass spectrometer equipped with an Agilent 1200 Series Quaternary LC system. HR-electrospray ionization (ESI)–MS spectra were acquired with an AB SCIEX Triple TOF 5600 System or an Agilent 6230 TOF LC/MS System.

Isotopic enrichment. Growth conditions for *Streptomyces* sp. NRRL30475 were as previously described (see Supplementary Note)[16]. A seed culture was incubated at 30 °C for 72 h, when 2 ml was used to inoculate 50 ml of fresh medium. After fermentation for 65 h, 25 mg of filter-sterilized L-[1-^{13}C]Leu, L- [$^{13}C5$,^{15}N]Met or L-[$^{13}C4$,^{15}N]Asp was added to each 250-ml flask containing 50 ml of medium. Fermentation was continued for an additional 72 h. Compound **5** was extracted and purified as previously described (see Supplementary Note). Percentage enrichment was calculated based on the theoretical and observed isotopic distribution of **5**.

Cloning for gene expression. Genes were cloned from genomic DNA using standard procedures (primers listed in Supplementary Table 1). The gel-purified PCR product for *mur24* or *mur23* was digested with *Nde*I-*Bam*HI and ligated to the identical sites of pXY200 to yield pXY200-*mur24* and pXY200-*mur23*, respectively. PCR integrity was confirmed by DNA sequencing. The gel-purified PCR product for *lipJ* was sequenced and inserted into a pET30Xa/LIC vector using ligation-independent cloning, following the provided protocol. The gene *sphL* was synthesized by Genscript and subcloned into a pET30Xa/LIC vector for expression.

Site-directed mutagenesis. A K234A point mutation of Mur24 and a K229A point mutation of LipJ were generated by PCR amplification with Q5, hot start, high-fidelity, DNA polymerase using pET30-*mur24* or pET30-*lipJ* as a template, respectively. The template pET30-*mur24* was obtained using ligation-independent cloning with a pET30Xa/LIC vector following the provided protocol. The PCR product was digested with 10 units *Dpn*I for 2 h at 37 °C and transformed into *E. coli* NEB5α-competent cells. The sequence of the entire gene, with the introduction of the correct point mutation, was confirmed by sequencing. Plasmid pET30-*mur24*(K234A) was digested with *Nde*I-*Bam*HI, and the DNA fragment of the expected size was purified and ligated to the identical sites of pXY200 to yield pXY200-*mur24*(K234A).

Recombinant protein production. Plasmids pXY200-*mur24*, pXY200-*mur24* (K234A) and pXY200-*mur23* were transformed into *S. lividans* TK24 using poly(ethylene glycol)-mediated protoplast transformation and plated on R2YE medium supplemented with 50 µg ml^{-1} of apramycin. After 6 d at 28 °C, positive transformants were confirmed by colony PCR using InstaGene Matrix from Bio-Rad and LA-Taq polymerase with GC buffer I. Positive strains were used to inoculate 50 ml R2YE medium containing 50 µg ml^{-1} of apramycin, grown for 3 d at 28 °C and 250*g*, and 2 ml transferred to 100 ml fresh R2YE mediium containing 50 µg ml^{-1} of apramycin. After growth for 3 d at 28 °C and 250*g*, protein expression was induced by the addition of thiostrepton (5 µg ml^{-1}) and the culture was incubated for another 24 h before harvesting. The cells from 400 ml of the culture were collected by centrifugation. The pellet was thoroughly resuspended in ice-cold buffer A (100 mM KH_2PO_4, 300 mM NaCl, 10 mM imidazole, pH 8.3) supplemented with 4 mg ml^{-1} of lysozyme which was subsequently added to the suspension. After incubation at 30 °C for 30 min, the cell suspension was mixed by pipetting and lysed using a Qsonica sonicator for a total of 8 min at 40% amplitude with 10-s pulses separated by 50-s rest periods. After centrifugation, the protein was purified using affinity chromatography with HisPur Ni-NTA agarose, and proteins were eluted with increasing concentrations of imidazole in buffer A. Purified proteins were concentrated and buffer exchanged into buffer B (25 mM KH_2PO_4, 100 mM NaCl, pH 8.3) using Amicon Ultra 10000 MWCO centrifugal filters and stored as glycerol stocks (40%) at −20 °C. Protein purity was assessed using sodium dodecylsulfate–12% poly(acrylamide) gel electrophoresis; His_6-tagged proteins were used without further modifications.

Plasmids pET30-*lipJ*, pET30-*lipJ*(K229A) and pET28a-*sphL* were introduced into BL21(DE3), and the transformed strains were grown in LB supplemented with 50 µg ml^{-1} of kanamycin or ampicillin. After inoculation of 500 ml lysogeny broth with 50 µg ml^{-1} of kanamycin or ampicillin, the cultures were grown at 37 °C until the cell density reached an $A_{600} \approx 0.5$, when expression was induced with 0.1 mM isopropyl β-D-1-thiogalactopyranoside. Cells were harvested and processed as described for Mur24.

Reactions with Mur28 and Mur24. Reaction mixtures consisted of 25 mM potassium phosphate (pH 8.3), 500 µM **8**, 500 µM AdoMet, 1 mM ATP, 1 mM $MgCl_2$, 100 µM PLP, and 200 nM Mur28 and Mur24 for 3 h at 30 °C, and the reaction was subsequently quenched by adding two volumes of acetonitrile followed by centrifugation (21,000*g*, 30 min) to remove the precipitated protein. The reaction was monitored by LC–MS or HPLC using a SeQuant ZIC-HILIC column (5 µm, 200 Å, 250 mm × 4.6 mm). A series of linear gradients was developed from 0.1% formic acid (mobile phase A) to acetonitrile with 0.1% formic acid (mobile phase B) in the following manner (beginning time and ending time with linear change to percentage B): 0–12 min, 80% B; 13–26 min, 50% B; 27–35 min, 80% B; 35–50 min, 80% B. The flow rate was kept constant at 0.4 ml min^{-1} and elution was monitored at 260 nm. Pre-column derivation with AQC, a derivatizing reagent for amines[53], was also used to detect **10**. The reaction product (20 µl) was mixed with 60 µl of 0.2 M sodium borate buffer (pH 8.8) and 20 µl of 3 mg ml^{-1} AQC–acetonitrile solution. The mixtures were incubated at 55 °C for 10 min and then allowed to cool to room temperature. The AQC-derivatized samples (50 µl) were analyzed by LC–MS using an Alltech Apollo C18 column (5 µm, 100 Å, 250 × 4.6 mm^2) with detection at 260 nm using mobile phases A and B. A gradient was applied as follows: linear gradient from 1% B to 20% B for 10 min, then to 60% B over 15 min, followed by a hold of 100% B for 5 min, then to 1% B for 5 min at a flow rate of 0.4 ml min^{-1}.

Reactions with Mur24 or LipJ. Reaction mixtures consisted of 25 mM potassium phosphate (pH 8.3), 500 µM **9**, 500 µM potential aminopropyl donor (AdoMet, SMM, L-VG or ACC), 100 µM PLP and 200 nM enzyme (Mur24, Mur24(K234A), LipJ, LipJ(K229A) or SphL for 6 h at 30 °C. The reaction was terminated by adding two volumes of cold acetonitrile, followed by centrifugation (21,000*g*, 30 min) to remove the precipitated protein. The reaction was monitored by LC–MS or HPLC using a SeQuant ZIC-HILIC column as described in Reactions with Mur28 and Mur24.

Purification of AdoMet isomers. The (*S*)- and (*R*)-forms of AdoMet were purified using HPLC[54] with a C18, reversed-phase, analytical column (Kinetex 5 µm, 100 Å, 250 mm × 4.6 mm from Phenomenex) using 50 mM ammonium acetate buffer (pH 5.4) with 1% trifluoroacetic acid.

Detection of α-ketobutyrate. Reaction mixtures consisted of 50 mM potassium phosphate (pH 8.3), 500 µM AdoMet, 100 µM PLP and 400 nM enzyme for 6 h at 30 °C, and the reaction was terminated by ultrafiltration using Amicon Ultra 3000 MWCO centrifugal filters. Samples were treated with MBTH as previously described[55]. In short, reaction mixtures (50 µl) were mixed with 50 µl of 1 M sodium acetate (pH 5.0) and 50 µl of 8 mM MBTH aqueous solution. The mixtures were then incubated at 50 °C for 30 min and analyzed using LC–MS with an analytical Thermo Scientific Acclaim 120 C18 column (5 µm, 120 Å, 100 mm × 4.6 mm) using mobile phases A and B. A gradient was applied as follows: linear gradient from 10% B to 40% B for 15 min, 40% B to 100% B for 10 min, followed by a hold of 100% B for 7 min, then to 10% D for 2 min at a flow rate of 0.4 ml min^{-1}. Elution was monitored at 325 nm.

UV/Vis spectral analysis. Absorbance spectra were recorded on a BioTek Synergy 2 Multi-Mode Microplate Reader using 30 µM indicated protein, with 1 mM of the respective substrates at 30 °C in buffer B supplemented with 100 µM PLP, 1 mM AdoMet, and 500 µM compound **9** or 500 µM compound **10**. Spectra were recorded every 1 min.

Activity of Mur24 with potential inhibitors. Reaction mixtures consisted of 25 mM potassium phosphate (pH 8.3), 250 µM **9**, 0.5 mM AdoMet, 100 µM PLP, potential inhibitors (2 mM L-VG, 1 mM sinefungin or 0.5 mM SMM) and 200 nM Mur24 for 3 h at 30 °C. The reactions were terminated by adding two volumes of cold acetonitrile followed by centrifugation. The reaction was monitored by LC–MS or HPLC using a SeQuant ZIC-HILIC column as described in Reactions with Mur28 and Mur24.

Reactions with hMAT2A and Mur24. The reaction mixture consisted of 50 mM potassium phosphate (pH 8.5), 50 mM KCl, 10 mM $MgCl_2$, 8 mM ATP, 1 mM L-Met, 40 µM PLP, 250 µM **9**, and 10 µM hMAT2A and 200 nM Mur24 for 3–6 h at 30 °C, and the reaction was subsequently quenched by adding two volumes of acetonitrile followed by centrifugation (21,000*g*, 30 min) to remove the precipitated

protein. The reaction components were analyzed by LC–MS using a SeQuant ZIC-HILIC column as described in Reactions with Mur28 and Mur24.

Reaction with Mur24 in D_2O. The reaction mixture (25 µl) consisted of 50 mM potassium phosphate (pH 8.5), 50 mM KCl, 10 mM $MgCl_2$, 8 mM ATP, 1 mM L-Met, 40 µM PLP, 250 µM **9**, 10 µM hMAT2A and 200 nM Mur24 for 6 h in D_2O (D_2O final percentage 80%) at 30 °C. Identical reactions were performed by starting directly with commercial AdoMet and consisted of 50 mM potassium phosphate (pH 8.5), 500 µM **9**, 1 mM AdoMet, 40 µM PLP and 200 nM enzyme Mur24 in D_2O (D_2O final percentage 80%) for 6 h at 30 °C. The reaction was also performed by starting with Mur24 product **10** and consisted of 50 mM potassium phosphate (pH 8.5), 500 µM **10**, 100 µM PLP and 200 nM enzyme Mur24 in D_2O (D_2O final percentage 80%) for the indicated time points at 30 °C. All reactions were quenched by adding two volumes of acetonitrile followed by centrifugation. The supernatant was dried, reconstituted in H_2O and incubated for 10 min before HR-ESI–MS analysis.

Activity of Mur23. Reaction mixtures consisted of 25 mM potassium phosphate (pH 8.3), 500 µM **10**, 100 µM PLP and 200 nM Mur23 for 1 h at 30 °C, and the reaction was terminated by adding two volumes of cold acetonitrile followed by centrifugation. For reaction mixtures containing calf intestinal phosphatase, they consisted of Cutsmart buffer, 25 mM potassium phosphate (pH 8.3), 500 µM **10**, 100 µM PLP, with or without 500 units ml^{-1} of calf intestinal phosphatase for 30 min at 37 °C. The reaction components were analyzed by LC–MS using a SeQuant ZIC-HILIC column as described in **Reactions with Mur28 and Mur24**.

Kinetics of Mur23 and Mur24. Reaction mixtures consisted of 25 mM potassium phosphate (pH 8.3), 100 µM PLP and almost-saturating AdoMet (2 mM) with variable compound **9** (5–500 µM). The reaction was performed at 30 °C with 200 nM Mur24 for 180 min and analyzed under initial velocity conditions. For Mur23, reactions consisted of 25 mM potassium phosphate (pH 8.3) and 100 µM PLP with variable compound **10** (5–1,000 µM). The Mur23-catalyzed reaction was performed at 30 °C with 50 nM Mur23 for 60 min and analyzed under initial velocity conditions (<10% conversion). Product formation was determined using HPLC with the gradient described above. Each data point represents a minimum of three replicate end-point assays; kinetic constants were obtained by nonlinear regression analysis using GraphPad Prism .

Reporting summary. Additional information on the research design is available in the Nature Research Reporting Summary linked to this article.

Data availability

All plasmids and raw data are available upon request. Sequences are deposited at National Center for Biotechnology Information under accession nos.: Mur24, ADZ45336; Mur23, ADZ45335; LipJ, BAJ05886; and SphL, BAO20191.

References

51. Spork, A. P., Koppermann, S., Dittrich, B., Herbst-Irmer, R. & Ducho, C. Efficient synthesis of the core structure of muraymycin and caprazamycin nucleoside antibiotics based on a stereochemically revised sulfur ylide reaction. *Tetrahedron Asymmetry* **21**, 763–766 (2010).
52. Hirano, S., Ichikawa, S. & Matsuda, A. Total synthesis of caprazol, a core structure of the caprazamycin antituberculosis antibiotics. *Angew. Chem. Int. Ed.* **44**, 1854–1856 (2005).
53. Cohen, S. A. & Michaud, D. P. Synthesis of a fluorescent derivatizing reagent, 6-aminoquinolyl-*N*-hydroxysuccinimidyl carbamate, and its application for the analysis of hydrolysate amino acids via high-performance liquid chromatography. *Anal. Biochem.* **211**, 279–287 (1993).
54. Zhang, J. & Klinman, J. P. High-performance liquid chromatography separation of the (*S*,*S*)- and (*R*,*S*)-forms of *S*-adenosyl-l-methionine. *Anal. Biochem.* **476**, 81–83 (2015).
55. Tanaka, H., Yamamoto, A., Ishida, T. & Horiike, K. Simultaneous measurement of D-serine dehydratase and D-amino acid oxidase activities by the detection 2-oxo-acid formation with reverse-phase high performance liquid chromatography. *Anal. Biochem.* **362**, 83–88 (2007).

Acknowledgements

This work was supported in part by the National Institutes of Health (NIH, grant nos. AI087849 and GM115261), the National Center for Advancing Translational Sciences (grant nos. UL1TR000117 and UL1TR001998), the Deutsche Forschungsgemeinschaft (grant no. DU1095/5-1), the state of Lower Saxony (Lichtenberg doctoral fellowship (CaSuS program) for A.L.), the Konrad-Adenauer-Stiftung (doctoral fellowship for D.W.) and the Fonds der Chemischen Industrie (doctoral fellowship for G.N.). NMR (600 MHz) data were collected at the NMR facility of the Center for Environmental Systems Biochemistry supported in part by the NIH (grant no. DK097215). We thank the Department of Pharmaceutical Sciences and the College of Pharmacy for financial support for MS and NMR instrumentation.

Author contributions

Z.C. and J.O. performed and analyzed the data for cloning, heterologous expression, and protein functional assignments and biochemical characterization. Z.C., X.W. and M.B. performed MS and NMR spectroscopy of enzymatic products and analyzed the respective data. X.L, Y.Z., A.L., D.W. and G.N. performed the chemical synthesis and analyzed the respective data. Z.C., J.S.T., C.D. and S.G.v.L. conceived the study, directed and planned the research, analyzed the data and wrote the article.

Competing interests

The authors declare no competing interests.

Additional information

Supplementary information is available for this paper at https://doi.org/10.1038/s41589-020-0548-3.

Correspondence and requests for materials should be addressed to S.G.V.L.

Reprints and permissions information is available at www.nature.com/reprints.

nature research

Corresponding author(s): Van Lanen, SG

Last updated by author(s): Mar 8, 2020

Reporting Summary

Nature Research wishes to improve the reproducibility of the work that we publish. This form provides structure for consistency and transparency in reporting. For further information on Nature Research policies, see Authors & Referees and the Editorial Policy Checklist.

Statistics

For all statistical analyses, confirm that the following items are present in the figure legend, table legend, main text, or Methods section.

n/a	Confirmed	
☐	☒	The exact sample size (*n*) for each experimental group/condition, given as a discrete number and unit of measurement
☐	☒	A statement on whether measurements were taken from distinct samples or whether the same sample was measured repeatedly
☐	☒	The statistical test(s) used AND whether they are one- or two-sided *Only common tests should be described solely by name; describe more complex techniques in the Methods section.*
☒	☐	A description of all covariates tested
☒	☐	A description of any assumptions or corrections, such as tests of normality and adjustment for multiple comparisons
☒	☐	A full description of the statistical parameters including central tendency (e.g. means) or other basic estimates (e.g. regression coefficient) AND variation (e.g. standard deviation) or associated estimates of uncertainty (e.g. confidence intervals)
☒	☐	For null hypothesis testing, the test statistic (e.g. *F*, *t*, *r*) with confidence intervals, effect sizes, degrees of freedom and *P* value noted *Give P values as exact values whenever suitable.*
☒	☐	For Bayesian analysis, information on the choice of priors and Markov chain Monte Carlo settings
☒	☐	For hierarchical and complex designs, identification of the appropriate level for tests and full reporting of outcomes
☒	☐	Estimates of effect sizes (e.g. Cohen's *d*, Pearson's *r*), indicating how they were calculated

Our web collection on statistics for biologists contains articles on many of the points above.

Software and code

Policy information about availability of computer code

Data collection	Agilent Mass Hunter Qualitative Analysis v B.08.00 for LCMS or AB SciEx Analyst TF 1.7 for LCMSMS; VNMR v 4.2 revision A or TopSpin v 4 for NMR.
Data analysis	GraphPad Prism 8.1 for kinetic analysis; Agilent Mass Hunter Qualitative Analysis v B.08.00 for LCMS or AB SciEx Analyst TF 1.7 for LCMSMS; MestReNova v 12.02.20910 for NMR; Geneious v 7.1.9 using Blosum45 for sequence alignment and phylogenetic analysis

For manuscripts utilizing custom algorithms or software that are central to the research but not yet described in published literature, software must be made available to editors/reviewers. We strongly encourage code deposition in a community repository (e.g. GitHub). See the Nature Research guidelines for submitting code & software for further information.

Data

Policy information about availability of data

All manuscripts must include a data availability statement. This statement should provide the following information, where applicable:

- Accession codes, unique identifiers, or web links for publicly available datasets
- A list of figures that have associated raw data
- A description of any restrictions on data availability

Provide your data availability statement here.

Field-specific reporting

Please select the one below that is the best fit for your research. If you are not sure, read the appropriate sections before making your selection.

☒ Life sciences ☐ Behavioural & social sciences ☐ Ecological, evolutionary & environmental sciences

Life sciences study design

All studies must disclose on these points even when the disclosure is negative.

Sample size	N/A
Data exclusions	N/A
Replication	Duplicates or Triplicates
Randomization	N/A
Blinding	N/A

Reporting for specific materials, systems and methods

We require information from authors about some types of materials, experimental systems and methods used in many studies. Here, indicate whether each material, system or method listed is relevant to your study. If you are not sure if a list item applies to your research, read the appropriate section before selecting a response.

Materials & experimental systems

n/a	Involved in the study
☒	☐ Antibodies
☒	☐ Eukaryotic cell lines
☒	☐ Palaeontology
☒	☐ Animals and other organisms
☒	☐ Human research participants
☒	☐ Clinical data

Methods

n/a	Involved in the study
☒	☐ ChIP-seq
☒	☐ Flow cytometry
☒	☐ MRI-based neuroimaging